Chapter 5

Energy Calibration of CsI(Tℓ) Counters

5.1 Introduction

Although CsI(Tℓ) calorimeter has an excellent intrinsic energy resolution as will be discussed later, the crystals have variation of the light output. Therefore we need to know the response of each counter for a fixed amount of energy deposit in order to convert a signal from the CsI(Tℓ) to an energy measured in that counter. This is called a calibration and is important to get a good energy resolution from the whole system of the electromagnetic calorimeter.

We calibrated all produced counters by cosmic ray muon before installing the counter into the container. This served as a final test of the counter before installation, and gave us a pre-calibration of light output to be used at the beginning of the experiment.

In the BELLE experiment, the CsI(Tℓ) counters will be calibrated by the electrons from the Bhabha scattering. We expect it will replace the cosmic-ray calibration and become the final and the most reliable calibration *in situ*.

The uniform light output from the CsI(Tℓ) crystal is important to the linearity of energy response. The good linearity is important for BELLE because the calibration obtained by Bhabha scattering at high energy must be used in much lower energy region where most of the gamma rays from B meson decay exist.

The uniformity of the light output along the crystal, which can not be measured by the Bhabha scattering, is also measured by the cosmic rays.

5.2 Setup

The layout of the cosmic ray stand which is used for the calibration is shown in Fig. 5.1. It consists of two sets of scintillation counters for triggering, an aluminum container box on the moving table to hold the crystals during the calibration, 8 layers of drift chambers for tracking cosmic ray and a layer of 5 cm thick lead for absorbing soft component of the cosmic ray. Twenty CsI(Tℓ) counters are placed horizontally at the predefined positions in the aluminum box and the box is inserted between the drift chambers for the measurement.

Each drift chamber has a sensitive area of 1.2 $\times$ 1.2 m^2 and consists of 12 drift cells with the cross section of 5 cm $\times$ 10 cm and the length of 1.2 m. It is made of 3 mm thick extruded aluminum. A Copper-Beryllium anode wire of 100 μm diameter was strung at the center of the cell. Two sets of four layer drift chambers sandwiched the aluminum container box with a configuration of X-X-Y-Y and Y-Y-X-X for the optimum tracking. The X and Y direction is defined in Fig. 5.1.

The chamber was operated with PR gas (Ar 90% + CH_4 10%) flushed at the rate of 100 cc/min. The signal from the anode wire is amplified and discriminated and the drift time was measured by LRS2277 CAMAC TDC's. The position resolution of 1.2 mm is obtained, which is sufficient to track the cosmic ray muon through the CsI(Tℓ) crystal and determine the path length inside the crystal.

The signal from the preamplifier was shaped with 1 μs time constant and converted to a time signal by HOHSHIN-HE2550 shaper/QT module. The time was digitized by LRS2277.

A complete electronics channel from the shaper/QT to the TDC was calibrated for each channel by using a reference counter. The difference between channels were approximately 1.5% and was corrected in the subsequent analysis. The sensitivity and linearity were routinely checked by sending a test pulse to the preamplifier. A calibration module which was the prototype for the real experiment was used for the purpose.

The electronics noise was estimated by the width of the pedestal and the average value was 216 keV.

The cosmic ray event was triggered by the coincidence of upper and lower layer of the scintillation counters. The pulse height of CsI(Tℓ) counter and the timing information of the drift chamber were recorded by the Sun workstation[64]. The event with no hit in the CsI(Tℓ) counter was immediately discarded and the rest was used for the tracking. The vector of the muon was passed to the GEANT program and the

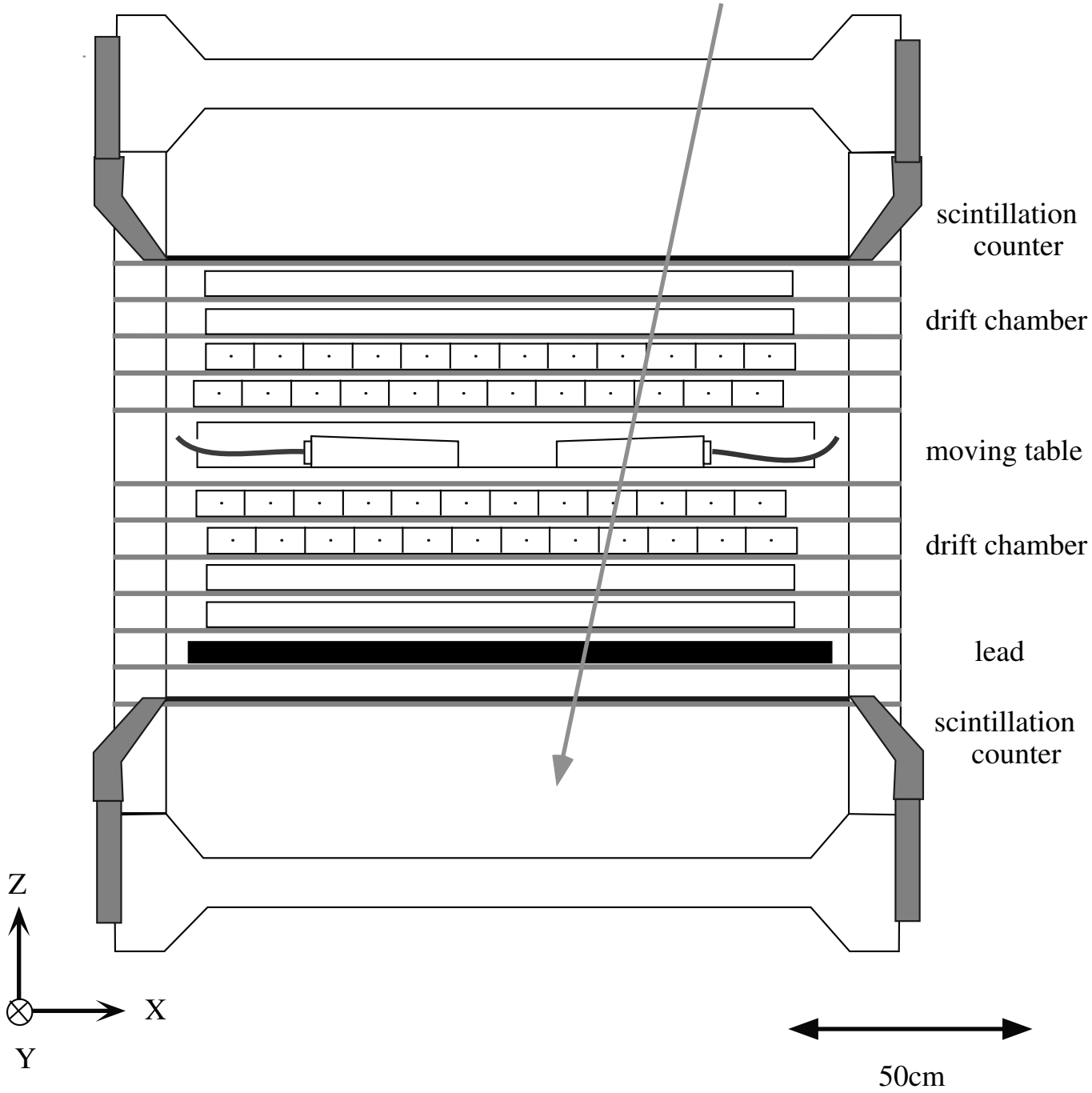

Figure 5.1: Cosmic ray stand.

path length in CsI was calculated on line using the GEANT tracking package. The value of pedestals are measured every 30 minutes and the most recent one was used for the analysis. The system covered a solid angle of 0.79 steradian at the center of the container box. The system was placed in an underground experimental hall and the trigger rate of the scintillation counter was 50 Hz, out of which about 5 % was useful for the calibration. The dead time for the data acquisition was approximately 75 %.

5.3 Analysis

In order to measure the uniformity of light output along the long axis of the crystal (z-axis), events were split into 9 subparts according to the z-value of impact point in the median plane (y=0) of the crystal. Each subparts has 3 cm wide acceptance in z. 1.5 cm at both ends of the crystal were not used (Fig. 5.2(a)). The cosmic ray which entered into the subpart with the polar angle more than 45 degrees or the one with less than 3 cm path length were excluded from the analysis. We plotted the pulse height of each subpart after correcting the difference of path length inside the crystal. An example of the pulse height normalized to the 1 cm path length is shown in Fig. 5.2(b).

The most probable channel (peak) of this distribution was obtained by fitting with the logarithmic Gaussian function $F(x)$ defined as follows;

$$F(x) = N \exp(-\frac{1}{2\sigma_0^2}\ ln^2(1 - \frac{x - x_p}{\sigma_E}\eta) - \frac{\sigma_0^2}{2}) \tag{5.1}$$

where x_p is peak value, η is asymmetry parameter, N is normalization factor and and σ_0 is $\frac{2}{\xi} sinh^{-1}(\frac{\eta\xi}{2})$. From this formula, the resolution of σ_E is calculated as the full width at half maximum (FWHM) divided by $\xi = 2\sqrt{ln4}$;

$$\sigma_E = \frac{FWHM}{\xi} \tag{5.2}$$

The number of cosmic rays used to determine the peak was about 500 events for each subpart. We estimate the error of light output in each subpart is approximately 2 % from the fluctuation among 9 subparts (see Fig 5.3). The statistical error is $\sim$ 0.5 %.

5.4 Energy Scale

The distribution obtained so far is in the unit of TDC counts/path length (counts/cm) in CsI. We will now scale it to a more general unit of N_{eh}/MeV, which is the number of

(a)

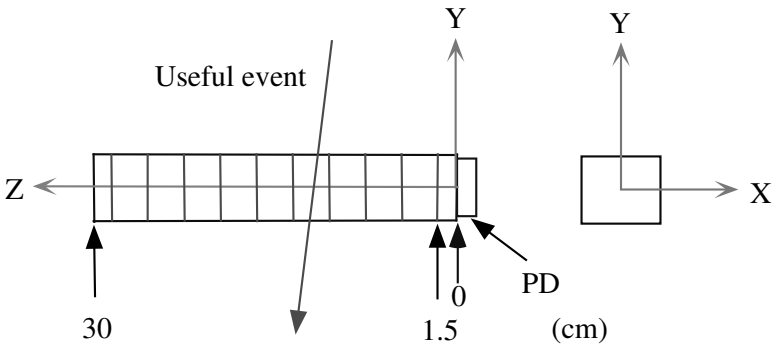

(b)

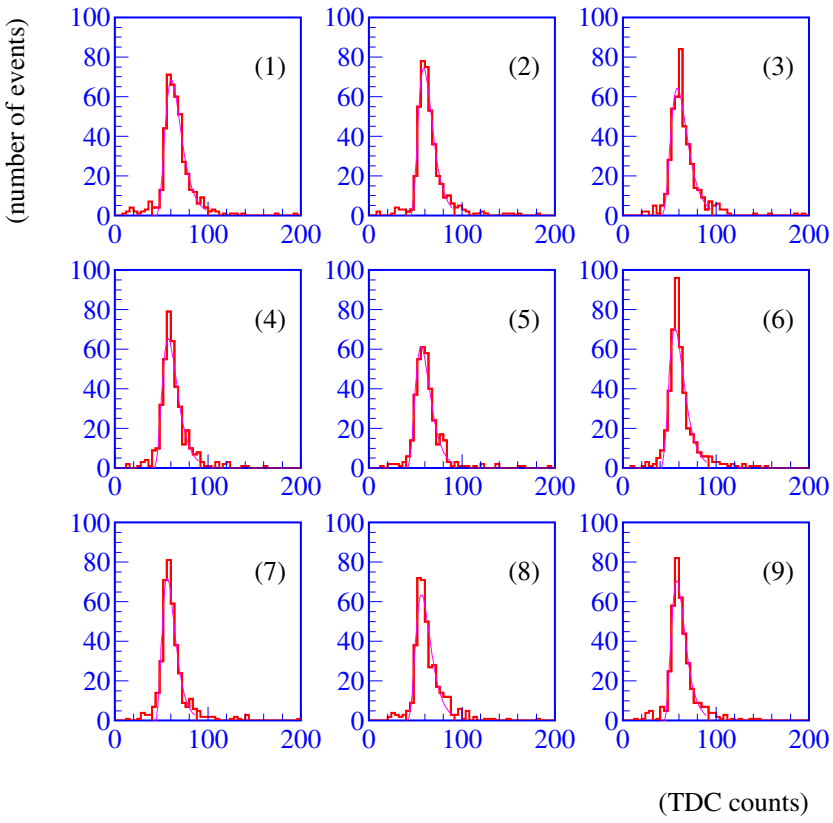

Figure 5.2: (a)Definition of CsI(Tℓ) crystal subparts and (b)the distribution of TDC counts/cm in 9 subparts.

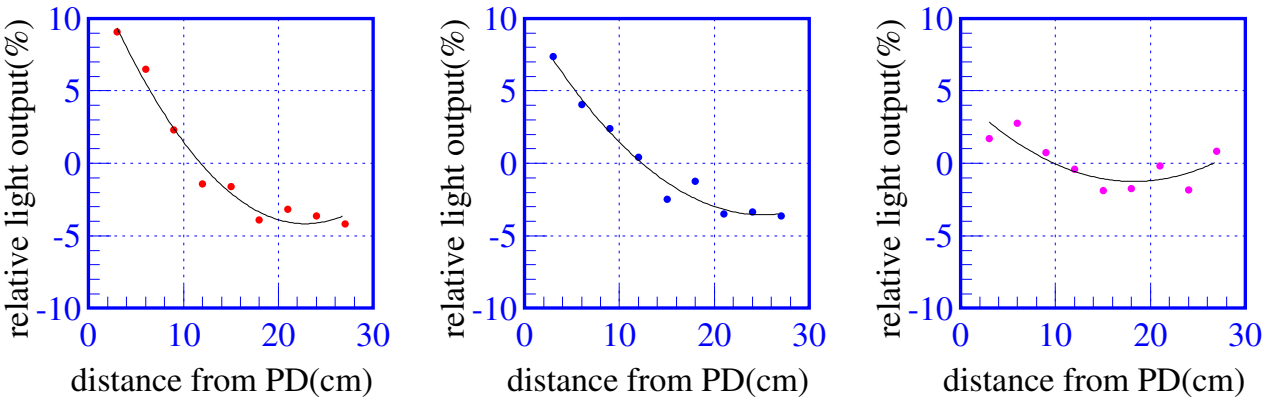

Figure 5.3: Examples of the uniformity of the light output for 9 subparts. The solid line is the fitting by the 3rd order polynomial.

electron-hole pairs detected in the photodiode for 1 MeV energy deposit in the crystal.

We first estimate an average energy deposited by the cosmic ray when cosmic muon passes through the CsI(Tℓ) crystal by using GEANT simulation. The energy loss of μ^- impinging perpendicularly to the 5.4 cm thick flat CsI plate was calculated at 22 energy points between 0.2 GeV and 1 TeV and its peak value was tabulated. Fig. 5.4(a) shows the results. The expected distribution of the energy loss by cosmic ray was calculated by weighting the tabulated energy loss by the measured momentum distribution of the cosmic ray [63] (see Fig. 5.4(b)). The result is 5.76 MeV for 1 cm path length in CsI.

We next find the relation between the TDC count and the number of photoelectrons. We detached the photodiode and preamplifier from the crystal and measured the TDC distribution of cosmic rays directly passing through the photodiode. The result is shown in Fig. 5.5(a). A corresponding GEANT simulation is shown in Fig. 5.5(b). The thickness of 300 μm is assumed for the photodiode and the effect of injection angle of the cosmic ray is included in the simulation. The peak of GEANT distribution is converted to electron-hole pairs as;

$$0.08363(\mathrm{MeV}) \div 3.6(\mathrm{eV}) = 23.23 \times 10^3(\text{electron hole pairs}) \tag{5.3}$$

where 3.6 eV is the necessary energy to create one electron-hole pair in Si photodiode. The conversion factor between the TDC counts and the electron-hole pairs is calculated from the above calculation and the peak value of the TDC distribution.

Another method is to use ^{241}Am radioactive source. We irradiated the photodiode directly by the 60 keV X-rays from ^{241}Am and recorded its pulse height. The mean

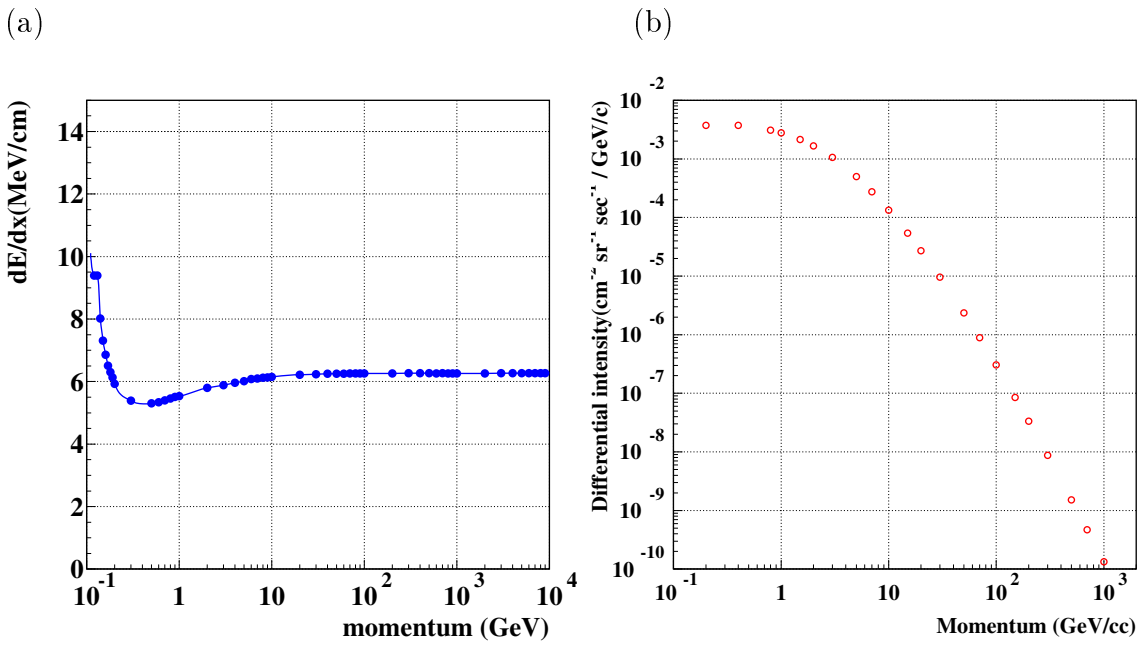

Figure 5.4: (a)Most probable energy deposit of cosmic ray in CsI counter (GEANT simulation). (b)The differential intensity of the cosmic ray.

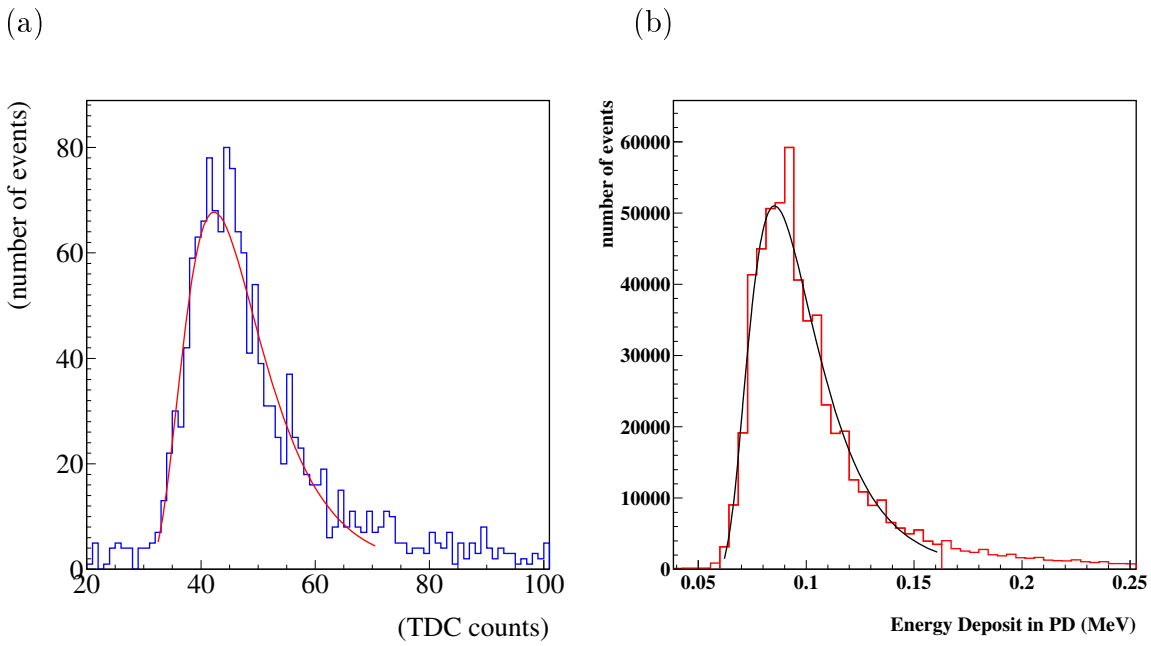

Figure 5.5: Energy deposit of cosmic rays in a photodiode (a)data and (b)GEANT simulation.

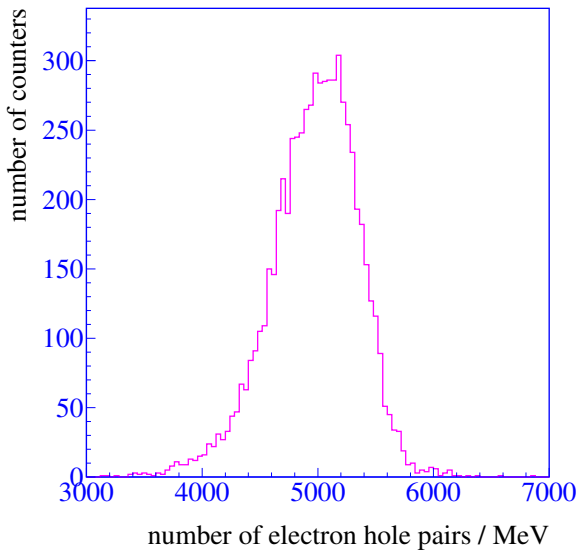

Figure 5.6: Results of the light output for all CsI(Tℓ) counters

value of this distribution corresponds to the number of electron-hole pairs of 16.7 $\times$ 10^3. This result was consistent within 4 % with the cosmic ray measurement.

5.5 Light Output Result

We measured the light output of all the barrel CsI(Tℓ) crystals (6,624 pieces). These were delivered from Budker Institute of Nuclear Physics (BINP), Russia, Shanghai Institute of Ceramics (SIC), China and Crismatec, France.

We defined the average of 9 subparts as the average light output of the crystal. The distribution of average light output for 6,624 barrel crystals is shown in Fig. 5.6. It is given in the unit of electron-hole pairs per 1 MeV of energy deposit in the crystal. The mean and rms of this distribution are 4,969 and 381 electron hole pairs. No significant difference was observed among the crystals of Crismatec, SIC and BINP.

In order to estimate the long term stability of the measurement, sample counters were measured again after 6 months from the first measurement. Fig. 5.7 shows the results. The peak shifts 1.4 % but the difference of light output is small within 1 % and the position dependence of light output also remain unchanged.

The result was compared with the average light output measured by ^{137}Cs. The data was obtained from the crystal acceptance test (see section 4.5.2). The comparison is shown in Fig. 5.8(a). There is a good agreement and the rms deviation of the ratio

(a) (b)

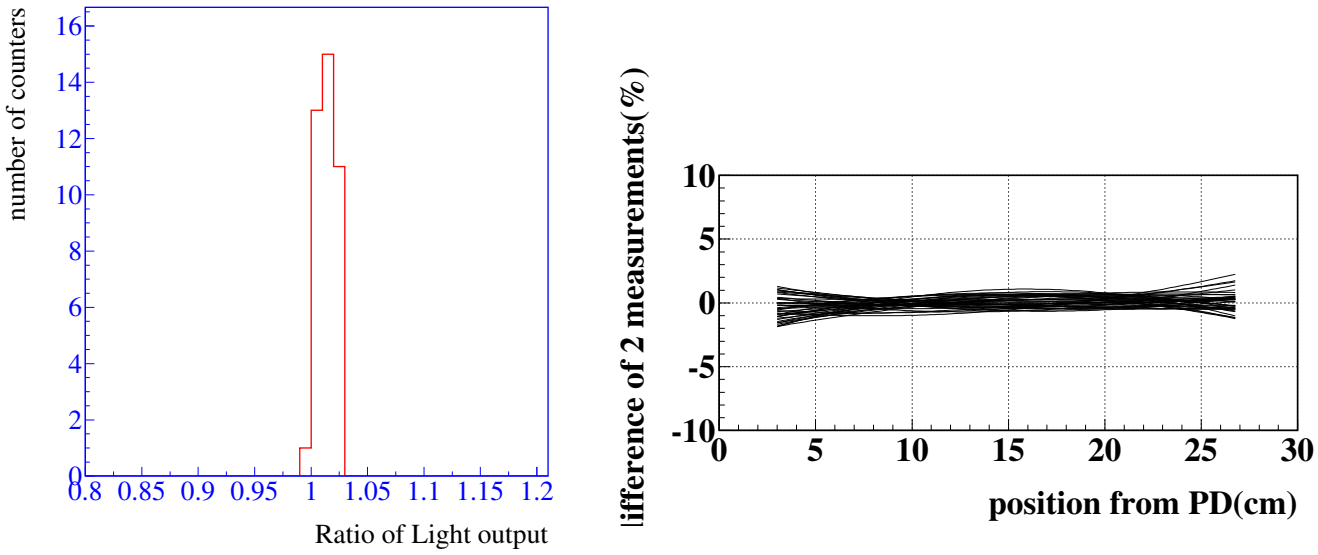

Figure 5.7: Reproducibility of (a)the light output and (b)position dependence after 6 months.

(a) (b)

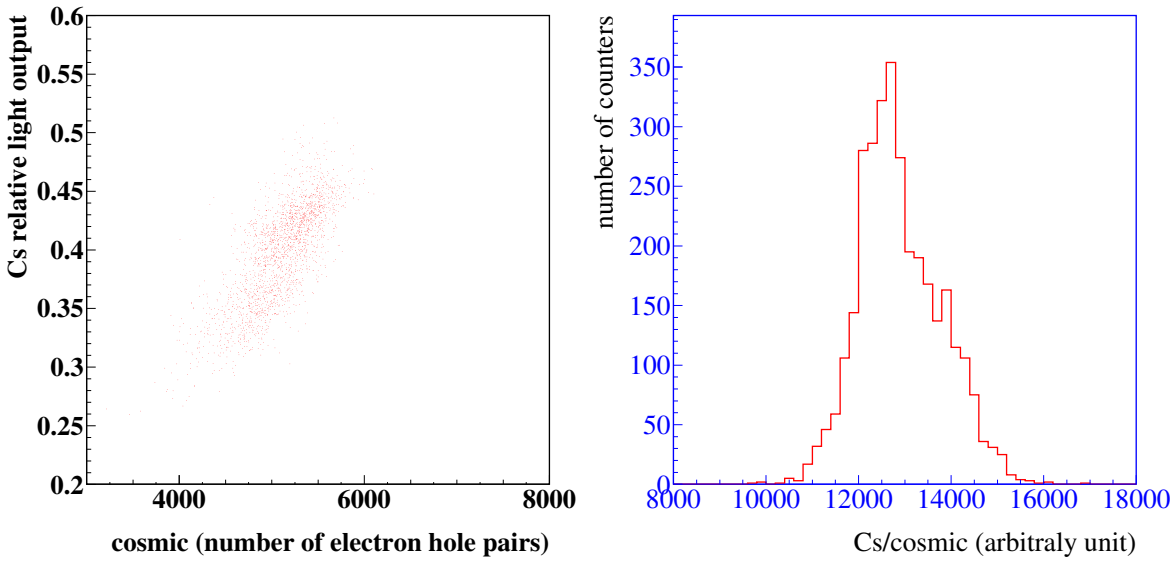

Figure 5.8: (a)Comparison between the calibration by cosmic rays and the ^{137}Cs source. (b)Ratio between two calibrations.

of two measurements is about 7 % (Fig. 5.8(b)).

5.6 Uniformity of Light Collection

The position dependence of the light output obtained from above measurements is shown in Fig. 5.9(a)-(c). The measurement of each subpart is normalized to the average light output and it is fitted by the 3rd order polynomial. The behaviors BINP crystal and Crismatec crystal are similar and the light output increases near the photodiode. The SIC crystals are separated in two types; one is similar with BINP/Crismatec and the other is almost flat over all regions of the counter.

The result of the measurement by the photomultiplier which is described in the previous chapter is shown in Fig. 5.9(d)-(f) for comparison. The difference between two measurements is shown in Fig. 5.9(g)-(i). A systematic shift between two measuring techniques is apparent. It is probably caused by the difference of optical contact; the photodiode is glued to the crystal and has a good optical contact, and in the phototube case, the light has to pass through the air layer and the rate of reflection at the boundary region is larger.

The distribution of uniformity parameter H (see 4.7) for barrel counters is shown in Fig. 5.10. The average was 9 %.

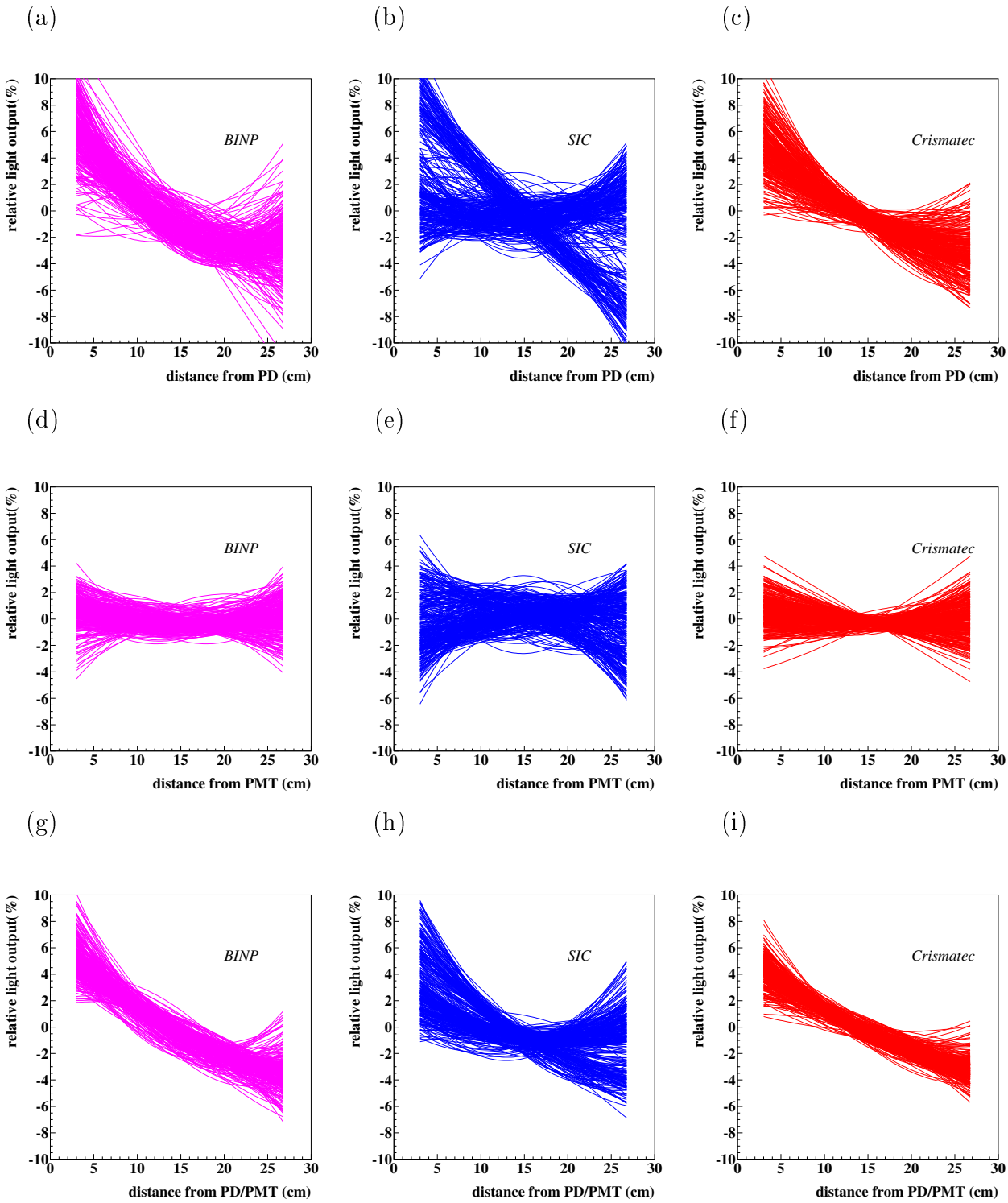

Figure 5.9: Position Dependence of light output. (a-c): Measurement by photodiode glued on the crystal. (d-f): Measurement by phototube with air gap. (g-i): Difference between two methods.

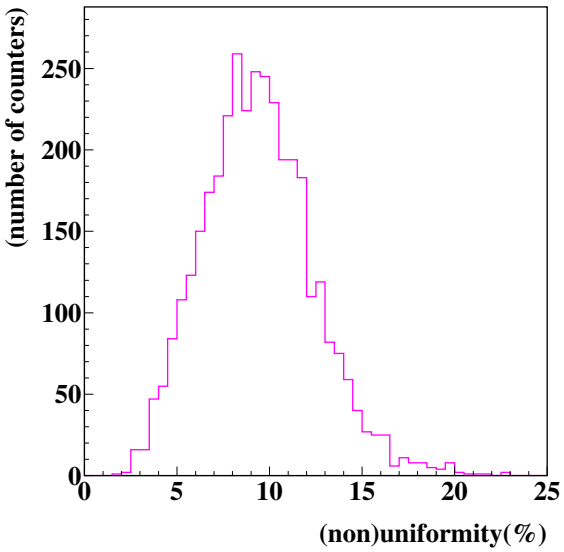

Figure 5.10: Distribution of uniformity.